

## Research Article

# Suppression of Chaos in Porous Media Convection under Multifrequency Gravitational Modulation

Karam Allali 

Laboratory of Mathematics and Applications, Faculty of Sciences and Technologies, University Hassan II of Casablanca, P.O. Box 146, Mohammedia, Morocco

Correspondence should be addressed to Karam Allali; [allalikaram@yahoo.fr](mailto:allalikaram@yahoo.fr)

Received 29 December 2017; Accepted 26 February 2018; Published 3 April 2018

Academic Editor: Giorgio Kaniadakis

Copyright © 2018 Karam Allali. This is an open access article distributed under the Creative Commons Attribution License, which permits unrestricted use, distribution, and reproduction in any medium, provided the original work is properly cited.

Suppression of chaos in porous media convection under multifrequency gravitational modulation is investigated in this paper. For this purpose, a two-dimensional rectangular fluid-saturated porous layer heated from below subjected to a vertical gravitational modulation will be considered. The model consists of nonlinear heat equation coupled with a system of equations describing the motion under Darcy law. The time-dependent gravitational modulation is assumed to be with two frequencies  $\sigma_1$  and  $\sigma_2$ . A spectral method of solution is used in order to reduce the problem to a system of four ordinary differential equations. The system is solved numerically by using the fifth- and a sixth-order Runge-Kutta-Verner method. Oscillating and chaotic convection regimes are observed. It was shown that chaos can be suppressed by appropriate tuning of the frequencies' ratio  $\eta = \sigma_2/\sigma_1$ .

## 1. Introduction

Several studies have been devoted to investigating the effect of a periodic gravitational modulation on the convective instability in a fluid layer. Indeed, the modulation of gravity can lead to stabilizing or destabilizing effect on the dynamics and the convective properties of the fluid [1, 2]. In practice, the gravitational modulation can be achieved by oscillating, in the vertical direction, the fluid container that is already subjected to a constant gravitational field. The modulation of gravity, with some specific amplitudes and frequencies, can contribute to the improvement of product performances such as solidification process [3, 4], frontal polymerization [5], or crystal growth [6].

The effect of gravitational modulation on natural convection in a porous layer was studied by Govender [7]. The linear stability analysis method was used to reduce the problem to a Mathieu equation and it was shown that increasing the frequency of vibration stabilizes the fluid convection. Elhajjar et al. [8] studied the influence of small-amplitude and high-frequency vertical vibrations on the Soret-driven convection flow. Both the direct numerical simulations and linear stability analysis were used in order to show that vibrations delay the transition from unicellular

to bicellular flow regime. More recently, Vadasz et al. [9, 10] studied the periodic and chaotic natural convection in a porous layer subject to vertical vibrations. It was shown that periodic and chaotic solutions alternate when Rayleigh number increases. All those previous works consider the effect of one frequency gravitational modulation. However, adding another frequency or more can change considerably the onset of convection regime. For instance, it was shown that the gravitational modulation with two incommensurate frequencies produces a convective stabilizing or destabilizing effect depending on the frequencies' ratio [11, 12]. In the absence of gravitational modulation, it was shown that chaos and thermal convection instabilities can be controlled or even suppressed by tuning of the temperature boundary values [13, 14].

Motivated by the recent works of Vadasz et al. [9, 10], the aim of this present paper is to continue the investigation of the influence of gravitational modulation on convective instability in porous layer heated from below, by assuming that the modulation is with two frequencies. To this end, we will consider that the system containing the fluid and the porous matrix are subjected to two-frequency vertical gravitational modulation. This external excitation causes a time-dependent acceleration given by  $g + b(t)$ , where  $g$  is

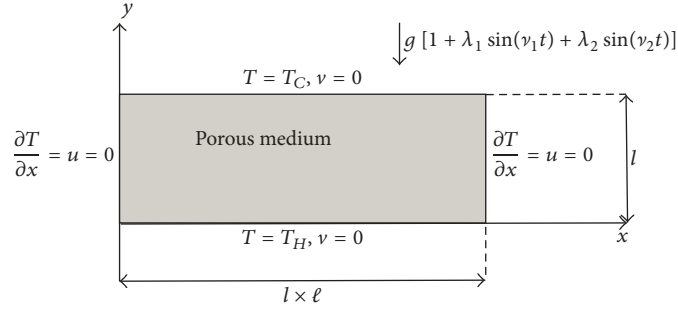


FIGURE 1: A two-dimensional rectangular porous domain heated from below subjected to two-frequency gravitational modulation.

the gravity acceleration and  $b(t) = \lambda_1 \sin(\nu_1 t) + \lambda_2 \sin(\nu_2 t)$ , where  $\lambda_1$  and  $\lambda_2$  and  $\nu_1$  and  $\nu_2$  are the amplitudes and the frequencies of the vibration, respectively. We will examine the effect of the two frequencies' ratio on the convective instability of the fluid flow and whether the chaos regime can be suppressed by tuning of the second frequency. Indeed, in many situations, chaos presents a troublesome phenomenon that may lead to physical system damage, thermal explosion due to irregular temperature oscillations, deadly epilepsy, and cardiac arrhythmias [15–18]. Accordingly, the need for chaos suppression is very important. Among those situations, one will be presented in this paper and we will study the effectiveness of introducing a second frequency gravitational modulation in chaos suppression. The need to add such second frequency gravitational modulation is particularly interesting when the first frequency is constrained to take some specific values or belongs to a narrow interval for which the chaos persists. In this paper, we will study the importance of adding a second frequency gravitational modulation in controlling chaos for both problems dealing with low or high Prandtl number fluids.

The paper is organized as follows: the next section introduces the model, while Section 3 deals with the numerical method used in our simulations. Results and discussions are provided in Section 4. The last section concludes the work.

## 2. Mathematical Formulation

**2.1. The Mathematical Model.** We consider a two-dimensional rectangular fluid-saturated porous layer subjected to a vertical gravitational modulation, as shown in Figure 1. We assume that the fluid is incompressible and is heated from below. The model of such a process can be described by the energy equation coupled with the hydrodynamics equations under the Boussinesq-Darcy approximation:

$$\begin{aligned} \frac{\partial T}{\partial t} + \mathbf{v} \cdot \nabla T &= \kappa \Delta T, \\ \frac{\partial \mathbf{v}}{\partial t} + \frac{\mu}{K} \mathbf{v} + \nabla p &= g\beta(T - T_C)(1 + \lambda_1 \sin(\nu_1 t) + \lambda_2 \sin(\nu_2 t))\boldsymbol{\gamma}, \\ \nabla \cdot \mathbf{v} &= 0, \end{aligned} \quad (1)$$

where  $T$  denotes the temperature,  $\mathbf{v} = (u, v)$  is the velocity,  $p$  is the pressure,  $\kappa$  is the coefficient of thermal diffusivity,  $\mu$  is the kinematic viscosity,  $g$  is the gravity,  $\boldsymbol{\gamma}$  is a unit vector in the downward vertical direction (in the sense of gravity),  $T_C$  is the cold wall temperature, and  $K$  is the permeability. We consider the following boundary conditions:

$$\begin{aligned} x &= 0, \ell \times l, \\ \frac{\partial T}{\partial x} &= u = 0, \\ v &= 0, \\ T &= T_C, \\ v &= 0, \\ y &= l, \\ T &= T_H, \\ v &= 0; \end{aligned} \quad (2)$$

here  $T_H$  is the hot wall temperature;  $\ell \times l$  and  $l$  are the horizontal and the vertical dimensions of the porous medium. The boundary conditions for the temperature correspond to the adiabatic (no-flux) condition at the lateral boundaries and fixed temperature at the lower and upper boundaries. For the velocity, its normal component at the boundary is zero. This means that the fluid does not intersect the boundary. In what follows, we will denote by  $\mathcal{D}T_c = T_H - T_C$  the characteristic temperature difference.

**2.2. The Dimensionless Model.** To obtain the dimensionless model, we introduce new spatial variables  $x' = x/l$  and  $y' = y/l$ , time  $t' = (\kappa/l^2)t$ , velocity  $(l/\kappa)\mathbf{v}$ , pressure  $(K/\mu\kappa)p$ , and the frequencies  $\sigma_i = (l^2/\kappa)\nu_i$  ( $i = 1, 2$ ). Denoting  $\theta = (T - T_C)/\mathcal{D}T_c$  and keeping for convenience the same notation for the other variables, we obtain

$$\frac{\partial \theta}{\partial t} + u \frac{\partial \theta}{\partial x} + v \frac{\partial \theta}{\partial y} = \frac{\partial^2 \theta}{\partial x^2} + \frac{\partial^2 \theta}{\partial y^2}, \quad (3)$$

$$\chi \frac{\partial u}{\partial t} + u + \frac{\partial p}{\partial x} = 0, \quad (4)$$

$$\chi \frac{\partial v}{\partial t} + v + \frac{\partial p}{\partial y} \quad (5)$$

$$= -R_a \theta (1 + \lambda_1 \sin(\sigma_1 t) + \lambda_2 \sin(\sigma_2 t)),$$

$$\frac{\partial u}{\partial x} + \frac{\partial v}{\partial y} = 0. \quad (6)$$

Here  $R_a = g\beta \mathcal{D} T_c K l / \kappa \mu$  is the Rayleigh number and  $(u, v)$  is the velocity vector. The parameter  $\chi = 1/Pr_D$  stands for the inverse of Darcy-Prandtl number with  $Pr_D = P_r/D_a$ ;  $P_r = \mu/\kappa$  is the Prandtl number and  $D_a = K/l^2$  is the Darcy number.

The system of (3)–(6) is supplemented by the free surface boundary conditions for the velocity, zero boundary condition for the temperature at the upper and lower boundaries of the rectangular domain, and adiabatic boundary condition at the side boundaries:

$$\begin{aligned} x &= 0, \ell, \\ \frac{\partial \theta}{\partial x} &= u = 0, \\ y &= 0, \\ \theta &= 0, \\ v &= 0, \\ y &= 1, \\ \theta &= 1, \\ v &= 0. \end{aligned} \quad (7)$$

### 3. The Spectral Method of Solution

In order to perform the mathematical analysis of our problem, we first introduce, due to the incompressibility property of the fluid, the stream function  $\psi$  defined by

$$\begin{pmatrix} u \\ v \end{pmatrix} = \begin{pmatrix} \frac{\partial \psi}{\partial y} \\ -\frac{\partial \psi}{\partial x} \end{pmatrix}. \quad (8)$$

We apply the rotational operator to the system of (4)–(5) in order to eliminate the pressure; the system becomes

$$\frac{\partial \theta}{\partial t} + \frac{\partial \psi}{\partial y} \frac{\partial \theta}{\partial x} - \frac{\partial \psi}{\partial x} \frac{\partial \theta}{\partial y} = \frac{\partial^2 \theta}{\partial x^2} + \frac{\partial^2 \theta}{\partial y^2}, \quad (9)$$

$$\left( \chi \frac{\partial \Delta \psi}{\partial t} + \Delta \psi \right) \quad (10)$$

$$+ Ra \frac{\partial \theta}{\partial x} (1 + \lambda_1 \sin(\sigma_1 t) + \lambda_2 \sin(\sigma_2 t)) = 0.$$

To apply the spectral method [19, 20], we will look for a solution of the problem in the form of the basic solution

added to a variation one. More precisely, we will separate the stream function and temperature into a basic conduction part and variation convection one in the form

$$\begin{aligned} \psi &= \psi_B + \psi_V = \psi_V, \\ \theta &= \theta_B + \theta_V = 1 - y + \theta_V, \end{aligned} \quad (11)$$

where  $\psi_B$  and  $\theta_B$  are the basic solution of problem (9)–(10). The variation part of the solution is chosen as follows:

$$\begin{aligned} \psi_V &= A_{11} \sin\left(\frac{\pi x}{\ell}\right) \sin(\pi y), \\ \theta_V &= B_{11} \cos\left(\frac{\pi x}{\ell}\right) \sin(\pi y) + B_{02} \sin(2\pi y). \end{aligned} \quad (12)$$

These two representations are equivalent to a Galerkin expansion of the solution in  $x$  and  $y$  directions, truncated when  $(i + j) = 2$ , where  $i$  and  $j$  are the Galerkin summation indices in  $x$ -direction and in  $y$ -direction, respectively. By substituting the form of solutions (11) in (10), we will have

$$\begin{aligned} -\left(\chi \frac{d}{dt} + 1\right) \left(\pi^2 \left(\frac{1}{\ell^2} + 1\right) A_{11} \sin\left(\frac{\pi x}{\ell}\right) \sin(\pi y)\right) \\ - Ra (1 + \lambda_1 \sin(\sigma_1 t) + \lambda_2 \sin(\sigma_2 t)) \left(\frac{\pi}{\ell} B_{11}\right) \\ \cdot \sin\left(\frac{\pi x}{\ell}\right) \sin(\pi y) = 0; \end{aligned} \quad (13)$$

by setting

$$\varrho = \frac{\ell^2}{\ell^2 + 1}, \quad (14)$$

we will have

$$\begin{aligned} \left\{ \frac{\pi^2 \chi}{\varrho} \frac{dA_{11}}{dt} + \frac{\pi^2}{\varrho} A_{11} \right. \\ \left. + \frac{\pi R_a}{\ell} (1 + \lambda_1 \sin(\sigma_1 t) + \lambda_2 \sin(\sigma_2 t)) B_{11} \right\} \\ \cdot \sin\left(\frac{\pi x}{\ell}\right) \sin(\pi y) = 0. \end{aligned} \quad (15)$$

Again, by substituting the form of solutions (11) in (9), we will have

$$\begin{aligned} \frac{dB_{11}}{dt} \cos\left(\frac{\pi x}{\ell}\right) \sin(\pi y) + \frac{dB_{02}}{dt} \sin(2\pi y) \\ - A_{11} B_{11} \frac{\pi^2}{\ell} \sin^2\left(\frac{\pi x}{\ell}\right) \sin(\pi y) \cos(\pi y) \\ + A_{11} \frac{\pi}{\ell} \cos\left(\frac{\pi x}{\ell}\right) \sin(\pi y) \end{aligned}$$

$$\begin{aligned}
& -A_{11}B_{11}\frac{\pi^2}{\ell}\cos^2\left(\frac{\pi x}{\ell}\right)\sin(\pi y)\cos(\pi y) \\
& -A_{11}B_{02}\frac{2\pi^2}{\ell}\cos\left(\frac{\pi x}{\ell}\right)\sin(\pi y)\cos(2\pi y) \\
& = -B_{11}\pi^2\cos\left(\frac{\pi x}{\ell}\right)\cos(\pi y) - 4B_{02}\pi^2\sin(2\pi y) \\
& -B_{11}\frac{\pi^2}{\ell^2}\cos\left(\frac{\pi x}{\ell}\right)\sin(\pi y),
\end{aligned} \tag{16}$$

which means

$$\begin{aligned}
& \frac{dB_{11}}{dt}\cos\left(\frac{\pi x}{\ell}\right)\sin(\pi y) + \frac{dB_{02}}{dt}\sin(2\pi y) \\
& -A_{11}B_{11}\frac{\pi^2}{2\ell}\sin(2\pi y) \\
& +B_{11}\frac{\pi^2}{\ell}\cos\left(\frac{\pi x}{\ell}\right)\sin(\pi y) \\
& -A_{11}B_{02}\frac{\pi^2}{\ell}\cos\left(\frac{\pi x}{\ell}\right)\sin(3\pi y) \\
& +A_{11}\frac{\pi}{\ell}\cos\left(\frac{\pi x}{\ell}\right)\sin(\pi y) + 4B_{02}\pi^2\sin(2\pi y) \\
& +A_{11}B_{02}\frac{\pi^2}{\ell}\cos\left(\frac{\pi x}{\ell}\right)\sin(\pi y) = 0;
\end{aligned} \tag{17}$$

then

$$\begin{aligned}
& \left(\frac{dB_{11}}{dt} + \frac{\pi^2}{\ell}B_{11} + \frac{\pi}{\ell}A_{11} + \frac{\pi^2}{\ell}A_{11}B_{02}\right)\cos\left(\frac{\pi x}{\ell}\right) \\
& \cdot \sin(\pi y) + \left(\frac{dB_{02}}{dt} - \frac{\pi^2}{2\ell}A_{11}B_{11} + 4\pi^2B_{02}\right) \\
& \cdot \sin(2\pi y) - \frac{\pi^2}{\ell}\cos\left(\frac{\pi x}{\ell}\right)\sin(3\pi y)A_{11}B_{02} = 0.
\end{aligned} \tag{18}$$

By multiplying (15) by  $\sin(\pi x/\ell)\sin(\pi y)$  and integrating over the space domain  $(0, 1) \times (0, \ell)$ , we have

$$\begin{aligned}
& \frac{\ell}{4}\left\{\frac{\pi^2\chi}{\ell}\frac{dA_{11}}{dt} + \frac{\pi^2}{\ell}A_{11}\right. \\
& \left. + \frac{\pi R_a}{\ell}(1 + \lambda_1\sin(\sigma_1 t) + \lambda_2\sin(\sigma_2 t))B_{11}\right\} = 0.
\end{aligned} \tag{19}$$

Again, multiplying (18) by  $\cos(\pi x/\ell)\sin(\pi y)$  and integrating over the space domain  $(0, 1) \times (0, \ell)$ , we will have

$$\frac{\ell}{4}\left(\frac{dB_{11}}{dt} + \frac{\pi^2}{\ell}B_{11} + \frac{\pi}{\ell}A_{11} + \frac{\pi^2}{\ell}A_{11}B_{02}\right) = 0. \tag{20}$$

Also, multiplying (18) by  $\sin(2\pi y)$  and integrating over the space domain  $(0, 1) \times (0, \ell)$ , it implies that

$$\frac{\ell}{2}\left(\frac{dB_{02}}{dt} - \frac{\pi^2}{2\ell}A_{11}B_{11} + 4\pi^2B_{02}\right) = 0, \tag{21}$$

so

$$\begin{aligned}
\frac{dA_{11}}{dt} & = -\frac{1}{\chi}\left(A_{11}\right. \\
& \left. + \frac{R_a}{\pi\zeta}(1 + \lambda_1\sin(\sigma_1 t) + \lambda_2\sin(\sigma_2 t))B_{11}\right), \\
\frac{dB_{11}}{dt} & = -\frac{\pi^2(\ell^2 + 1)}{\ell^2}\left(\frac{1}{\pi\zeta}A_{11} + B_{11} + \frac{1}{\zeta}A_{11}B_{02}\right), \\
\frac{dB_{02}}{dt} & = -\frac{\pi^2(\ell^2 + 1)}{\ell^2}\left(\frac{4\ell^2}{\ell^2 + 1}B_{02} - \frac{1}{2\zeta}A_{11}B_{11}\right).
\end{aligned} \tag{22}$$

The first equilibrium point of this system is

$$\begin{aligned}
A_{11}^f & = 0, \\
B_{11}^f & = 0, \\
B_{02}^f & = 0,
\end{aligned} \tag{23}$$

which is expected to be stable when  $R_a/\pi^2\zeta^2 < 1$ . However, for  $R_a/\pi^2\zeta^2 > 1$ , the following second equilibrium point is expected to be stable:

$$\begin{aligned}
A_{11}^* & = \pm\ell\sqrt{\frac{8R_a - 8\pi^2\zeta^2}{\pi^2\ell^2 + \pi^2}} = \pm\frac{2\sqrt{2}\sqrt{\ell}\sqrt{R_a}}{\pi}\sqrt{1 - \frac{\pi^2\zeta^2}{R_a}}, \\
B_{11}^* & = \pm\frac{\ell\pi\zeta}{R_a}\sqrt{\frac{8R_a - 8\pi^2\zeta^2}{\pi^2\ell^2 + \pi^2}} = \pm\frac{2\sqrt{2}\sqrt{\ell}\zeta}{\sqrt{R_a}}\sqrt{1 - \frac{\pi^2\zeta^2}{R_a}}, \\
B_{02}^* & = \frac{-R_a + \pi^2\zeta^2}{\pi R_a} = \frac{1}{\pi}\left(\frac{\pi^2\zeta^2}{R_a} - 1\right).
\end{aligned} \tag{24}$$

By assuming that

$$\frac{1}{R} = \frac{\pi^2\zeta^2}{R_a}, \tag{25}$$

we will have

$$\begin{aligned}
A_{11}^* & = \pm 2\sqrt{2}\sqrt{\ell}\zeta\sqrt{R-1}, \\
B_{11}^* & = \pm\frac{2\sqrt{2}\sqrt{\ell}\sqrt{R-1}}{\pi R}, \\
B_{02}^* & = -\frac{1}{\pi R}(R-1).
\end{aligned} \tag{26}$$

We set

$$\begin{aligned}
X & = -\left(\sqrt{2}\sqrt{\ell}\zeta\sqrt{R-1}\right)^{-1}A_{11}^*, \\
Y & = \left(\frac{2\sqrt{2}\sqrt{\ell}\sqrt{R-1}}{\pi R}\right)^{-1}B_{11}^*, \\
Z & = \left(-\frac{1}{\pi R}(R-1)\right)^{-1}B_{02}^*,
\end{aligned} \tag{27}$$

we obtain

$$\begin{aligned}\dot{X} &= -\frac{\varrho}{\chi\pi^2} (X - (1 + \lambda_1 \sin(\sigma_1 t) + \lambda_2 \sin(\sigma_2 t)) Y), \\ \dot{Y} &= -Y + RX - (R - 1) XZ, \\ \dot{Z} &= 4\varrho(XY - Z).\end{aligned}\quad (28)$$

By setting

$$\begin{aligned}\alpha &= \frac{\varrho}{\chi\pi^2}, \\ W &= \sigma_1 t,\end{aligned}\quad (29)$$

we will obtain the following system describing the problem dynamics:

$$\begin{aligned}\dot{X} &= -\alpha(X - Y) + \alpha(\lambda_1 \sin(W) + \lambda_2 \sin(\eta W)) Y, \\ \dot{Y} &= -Y + RX - (R - 1) XZ, \\ \dot{Z} &= 4\varrho(XY - Z), \\ \dot{W} &= \sigma_1,\end{aligned}\quad (30)$$

with the two modulation frequencies' ratio given by

$$\eta = \frac{\sigma_2}{\sigma_1}.\quad (31)$$

#### 4. Numerical Simulations

The system of (30) will be solved numerically using the fifth- and a sixth-order Runge-Kutta-Verner method. The used initial conditions are given as follows:

$$\begin{aligned}X_0 &= Y_0 = Z_0 = 0.9, \\ W_0 &= 0,\end{aligned}\quad (32)$$

and we will use the following parameters for all the numerical simulations:

$$\begin{aligned}\varrho &= 0.5, \\ \lambda_1 &= 1, \\ \lambda_2 &= 1.\end{aligned}\quad (33)$$

In order to compare our results with those in the work of Vadasz et al. [9], we will use the following parameter describing natural convection with low Prandtl number, that is,  $\alpha = 5$ . Meanwhile, to compare our results with the recent work taking into account high Prandtl number [10], we will fix  $\alpha = 500$ . The other control parameters  $R$ ,  $\sigma_1$ , and  $\eta$  will be varied adequately in order to check the impact of the two-frequency vibration on the behaviour of solution.

Figure 2 shows the projection of the solution on  $X$ - $Y$  and  $X$ - $Z$  planes for  $\alpha = 5$ ,  $R = 25$ ,  $\sigma_1 = 0$ , and  $\eta = 0$ . These parameters correspond to the absence of gravitational modulation case. The plots show chaotic behaviour of the

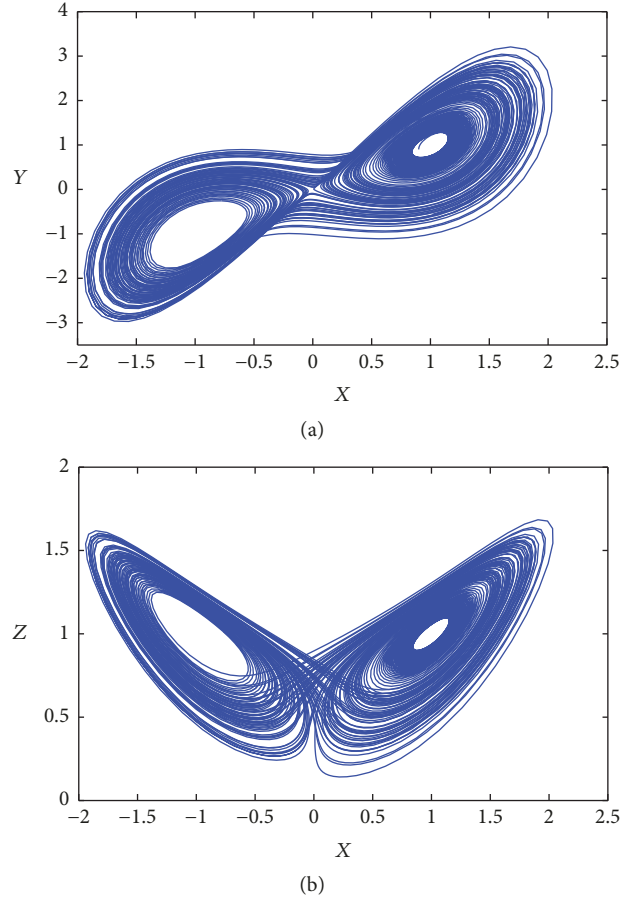


FIGURE 2: The solution on a phase diagram for  $\alpha = 5$ ,  $R = 25$ ,  $\sigma_1 = 0$ , and  $\eta = 0$ .  $Y$  versus  $X$  (a) and  $Z$  versus  $X$  (b).

solution, which are similar to those obtained in Vadasz et al. [9]. Figure 3 shows the behaviour of solution when the porous layer is subjected to one-frequency gravitational modulation; all the parameters in this figure are similar to the previous one, except  $\sigma_1 = 4.5$ . From this figure, it can be seen that the chaos still persists and the one-frequency gravitational modulation has no effect in controlling the chaos, since the leading Lyapunov exponent remains positive. Figure 4 shows a periodic convective regime, which means that suppression of chaos can be gained by changing one control parameter and making it nonzero:  $\eta = 6$ . One can conclude that the second gravitational modulation has a significant effect in chaos suppression. This result is confirmed by plotting the dynamics of the problem's Lyapunov exponents (see Figure 5). From this figure, we clearly see that all the problem's Lyapunov exponents are negatives, which support the periodicity behaviour of the convective regime. Hence, for the problems dealing with low-Prandtl number fluids, one can expect the suppression of chaos by introducing a second gravitational modulation frequency.

Figure 6 shows two projections from the phase diagram on both  $X$ - $Y$  and  $X$ - $Z$  planes for  $\alpha = 500$ ,  $R = 75$ ,  $\sigma_1 = 6.2$ , and  $\eta = 0$ . This case corresponds to one-frequency gravitational modulation and the plots are similar to those

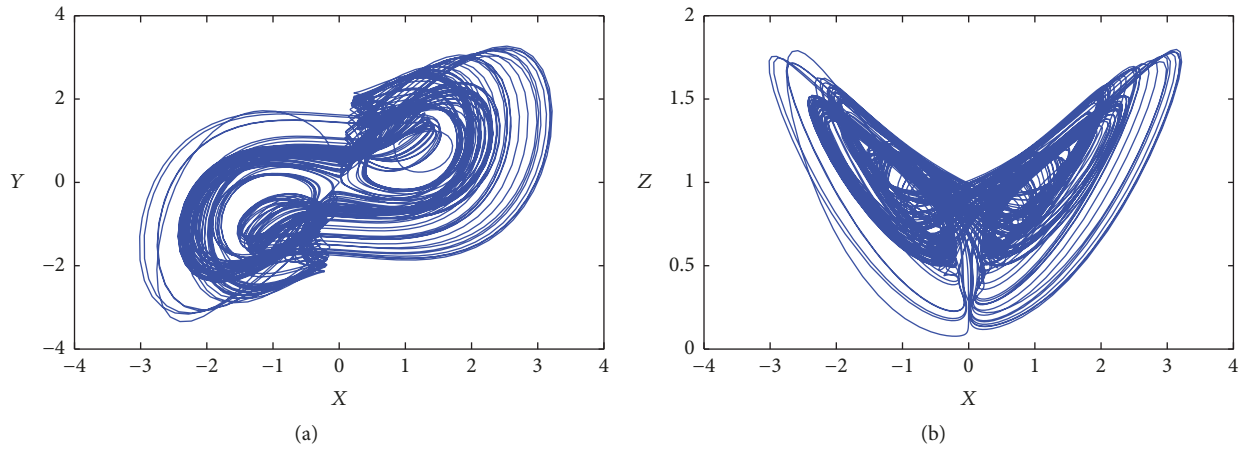


FIGURE 3: The solution on a phase diagram for  $\alpha = 5$ ,  $R = 25$ ,  $\sigma_1 = 4.5$ , and  $\eta = 0$ .  $Y$  versus  $X$  (a) and  $Z$  versus  $X$  (b).

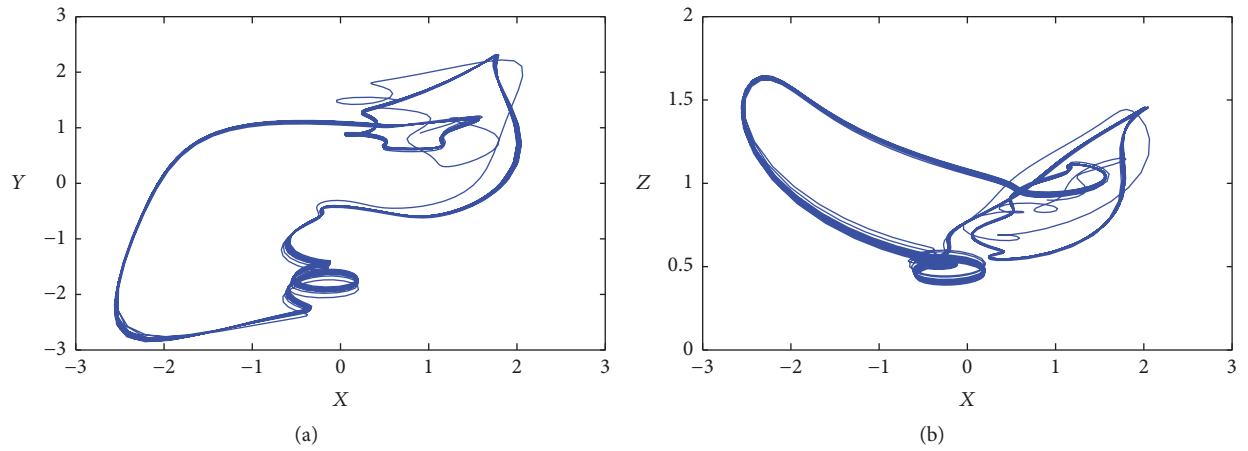


FIGURE 4: The solution on a phase diagram for  $\alpha = 5$ ,  $R = 25$ ,  $\sigma_1 = 4.5$ , and  $\eta = 6$ .  $Y$  versus  $X$  (a) and  $Z$  versus  $X$  (b).

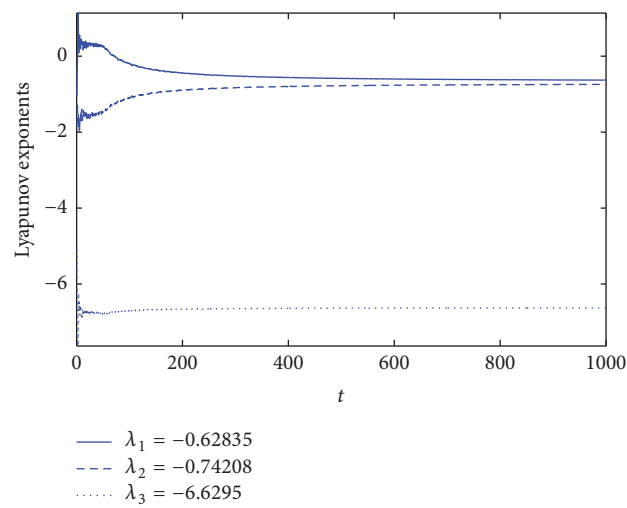


FIGURE 5: The dynamics of the problem's Lyapunov exponents for  $\alpha = 5$ ,  $R = 25$ ,  $\sigma_1 = 4.5$ , and  $\eta = 6$ .

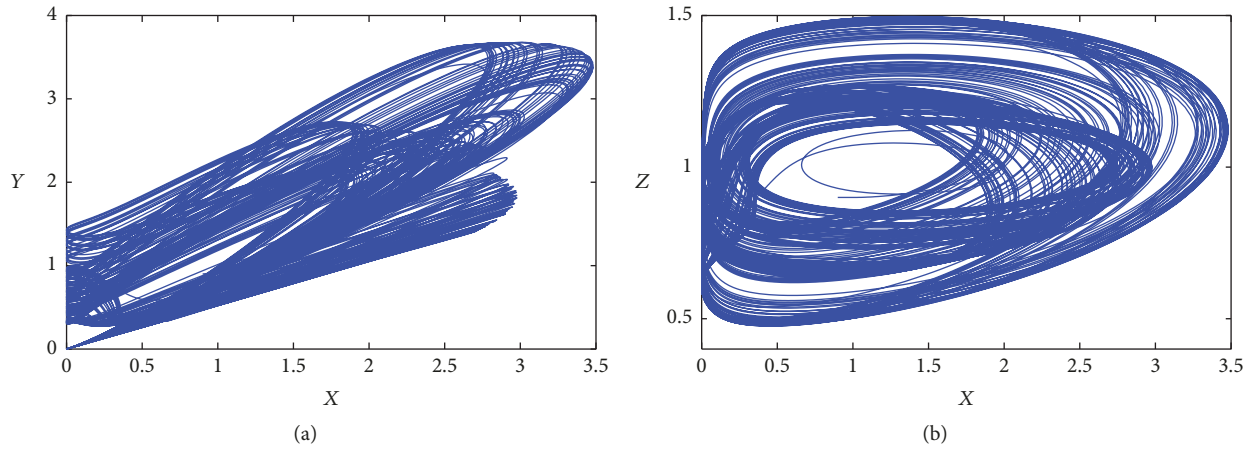


FIGURE 6: The solution on a phase diagram for  $\alpha = 500$ ,  $R = 75$ ,  $\sigma_1 = 6.2$ , and  $\eta = 0$ .  $Y$  versus  $X$  (a) and  $Z$  versus  $X$  (b).

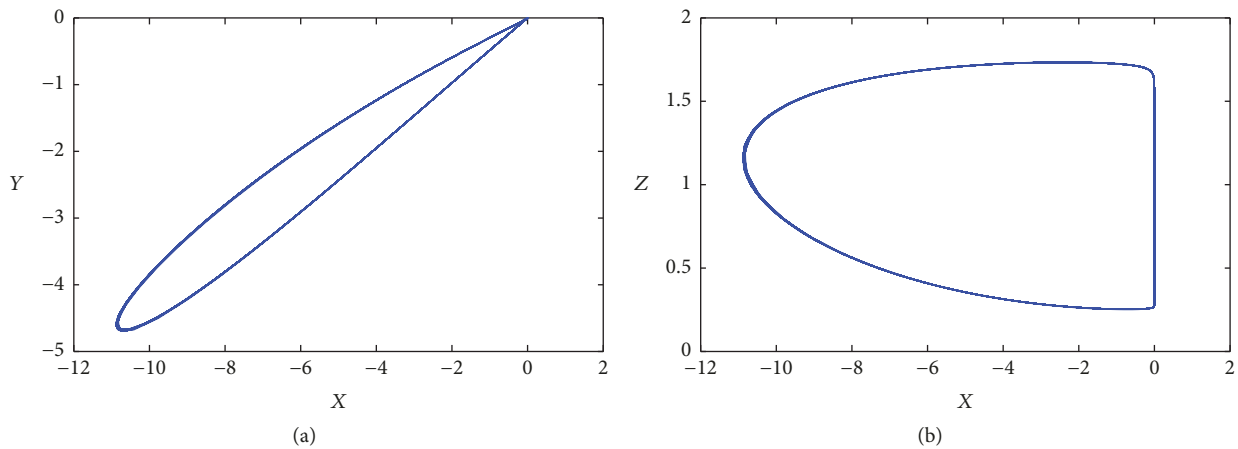


FIGURE 7: The solution on a phase diagram for  $\alpha = 500$ ,  $R = 75$ ,  $\sigma_1 = 6.2$ , and  $\eta = 3$ .  $Y$  versus  $X$  (a) and  $Z$  versus  $X$  (b).

obtained in Vadasz et al. [10]; this case corresponds to high-Prandtl number fluids. It can be seen from these two figures that the convective regime is chaotic. Figure 7 shows the behaviour of solution when the second modulation is introduced:  $\eta = 3$ ; the chaotic regime is completely suppressed for a second frequency greater only three times than the first one. It was found from the Lyapunov exponents' dynamics (not shown) that all the exponents are negatives, which confirms the chaos suppression. One can conclude that suppression of chaos can be achieved by looking only for small natural integer frequencies' ratio, which is more convenient to be reproduced experimentally.

## 5. Conclusion

In this paper, we have studied the effect of multifrequency gravitational modulation on chaos suppression in the problem dealing with natural convection in porous layer heated from below. For this purpose, we have assumed that the system containing the fluid and the porous matrix are subjected to two-frequency vertical gravitational modulation.

The considered model consists of heat equation coupled with the hydrodynamics equations under Darcy law. The mathematical analysis of the problem was performed by using the spectral method in order to reduce the problem to a system of four ordinary differential equations describing the dynamics of solution. The fifth- and a sixth-order Runge-Kutta-Verner method was used to solve numerically the reduced system of differential equations. Numerical simulations were conducted for both cases of low- and high-Prandtl number fluids. It was shown that the chaotic regime can be totally suppressed by choosing adequately the second gravitational modulation frequency. This situation happens when the frequencies' ratio is equal to six in the case of low Prandtl number or is equal to three in the case of high Prandtl number, which can be more convenient to be reproduced experimentally, since one can look only for small natural integer frequencies' ratio.

## Conflicts of Interest

The author declares that there are no conflicts of interest regarding the publication of this paper.

## References

- [1] T. B. Benjamin and F. Ursell, "The stability of the plane free surface of a liquid in vertical periodic motion," *Proceedings of the Royal Society A Mathematical, Physical and Engineering Sciences*, vol. 225, pp. 505–515, 1954.
- [2] P. M. Gresho and R. L. Sani, "The effects of gravity modulation on the stability of a heated fluid layer," *Journal of Fluid Mechanics*, vol. 40, no. 4, pp. 783–806, 1970.
- [3] P. Pelce and D. Rochwerger, "Parametric control of microstructures in directional solidification," *Physical Review A: Atomic, Molecular and Optical Physics*, vol. 46, no. 8, pp. 5042–5053, 1992.
- [4] J. Campbell, "Effects of vibration during solidification," *International Materials Reviews*, vol. 26, no. 1, pp. 71–108, 1981.
- [5] K. Allali, V. Volpert, and J. A. Pojman, "Influence of vibrations on convective instability of polymerization fronts," *Journal of Engineering Mathematics*, vol. 41, no. 1, pp. 13–31, 2001.
- [6] J. I. D. Alexander, J. Ouazzani, and F. Rosenberger, "Analysis of the low gravity tolerance of Bridgman-Stockbarger crystal growth. I. Steady and impulse accelerations," *Journal of Crystal Growth*, vol. 97, no. 2, pp. 285–302, 1989.
- [7] S. Govender, "Stability of convection in a gravity modulated porous layer heated from below," *Transport in Porous Media*, vol. 57, no. 1, pp. 113–123, 2004.
- [8] B. Elhajjar, A. Mojtabi, and M.-C. Charrier-Mojtabi, "Influence of vertical vibrations on the separation of a binary mixture in a horizontal porous layer heated from below," *International Journal of Heat and Mass Transfer*, vol. 52, no. 1-2, pp. 165–172, 2009.
- [9] J. J. Vadasz, J. P. Meyer, and S. Govender, "Vibration effects on weak turbulent natural convection in a porous layer heated from below," *International Communications in Heat and Mass Transfer*, vol. 45, pp. 100–110, 2013.
- [10] J. J. Vadasz, J. P. Meyer, and S. Govender, "Chaotic and periodic natural convection for moderate and high Prandtl numbers in a porous layer subject to vibrations," *Transport in Porous Media*, vol. 103, no. 2, pp. 279–294, 2014.
- [11] T. Boulal, S. Aniss, M. Belhaq, and A. Azouani, "Effect of quasi-periodic gravitational modulation on the convective instability in Hele-Shaw cell," *International Journal of Non-Linear Mechanics*, vol. 43, no. 9, pp. 852–857, 2008.
- [12] K. Allali, M. Belhaq, and K. El Karouni, "Influence of quasi-periodic gravitational modulation on convective instability of reaction fronts in porous media," *Communications in Nonlinear Science and Numerical Simulation*, vol. 17, no. 4, pp. 1588–1596, 2012.
- [13] Y. Z. Wang, J. Singer, and H. H. Bau, "Controlling chaos in a thermal convection loop," *Journal of Fluid Mechanics*, vol. 237, pp. 479–498, 1992.
- [14] J. Tang and H. H. Bau, "Feedback control stabilization of the no-motion state of a fluid confined in a horizontal porous layer heated from below," *Journal of Fluid Mechanics*, vol. 257, pp. 485–505, 1993.
- [15] J. Singer, Y.-Z. Wang, and H. H. Bau, "Controlling a chaotic system," *Physical Review Letters*, vol. 66, no. 9, pp. 1123–1125, 1991.
- [16] K. Allali, F. Bikany, A. Taik, and V. Volpert, "Numerical simulations of heat explosion with convection in porous media," *Combustion Science and Technology*, vol. 187, no. 3, pp. 384–395, 2015.
- [17] H. Zhang, D. Liu, and Z. Wang, *Controlling Chaos: Suppression, Synchronization and Chaotification*, Springer Science and Business Media, 2009.
- [18] B. B. Ferreira, A. S. De Paula, and M. A. Savi, "Chaos control applied to heart rhythm dynamics," *Chaos, Solitons & Fractals*, vol. 44, no. 8, pp. 587–599, 2011.
- [19] E. Magyari, "The Vadasz-Olek model regarded as a system of coupled oscillators," *Transport in Porous Media*, vol. 85, no. 2, pp. 415–435, 2010.
- [20] P. Vadasz and S. Olek, "Weak turbulence and chaos for low Prandtl number gravity driven convection in porous media," *Transport in Porous Media*, vol. 37, no. 1, pp. 69–91, 2000.



**Hindawi**

Submit your manuscripts at  
[www.hindawi.com](http://www.hindawi.com)

